Faculty of Physics, Astronomy and Applied Computer Science
Jagiellonian University

# Heat flow for harmonic maps between spheres

Paweł Biernat

Thesis written under the supervision of Prof. dr hab. Piotr Bizoń, submitted for the Master Degree in the Jagiellonian University

Cracow, June 2010

# Contents

# Chapter 1

# Introduction

Dirichlet energy $E(u) = \frac{1}{2}\int_M \|\nabla u\|^2 dV_M$ and its stationary points are central parts of many physical theories. We can generalize the Dirichlet energy to any map between differentiable manifolds endowed with inner products. Stationary points of such functional are called harmonic maps in analogy to harmonic functions, the main matter of this thesis are harmonic maps between spheres.

There is a powerful method available in the search for critical point of a functional $E$ called heat flow. The basic idea behind heat flow is to define a continuous vector field on the domain of a functional, such that the functional value decreases along its integral curves. Therefore, starting with any point as an initial state we can deform it along the vector field to reach a local minimum and thus, a stationary point. The heat flow realizes this idea by using an inverse gradient of $E$ as a vector field in which case integral curves are formally defined as solutions to

$$\partial_t F = -\delta E(F), \quad F(0) = F_0,$$

where $F_0$ is a starting point and $t$ is a parameter along the integral curve. The name "heat flow" is due to the fact that for the Dirichlet energy of the form $E(u) = \frac{1}{2}\int_M \|\nabla u\|^2 dV_M$ the heat flow turns out to be a heat equation. Proceeding with this analogy we will henceforth refer to the parameter $t$ as to time. One expects that the flow will asymptotically converge to the stationary point of $E$ where the gradient is zero. This approach has been successfully used by Eells and Sampson [3] to prove the existence of harmonic maps to manifolds of non positive sectional curvature.

If there are two local minima of $E$, by the continuity of the vector field there exist points which do not flow to either of them, which stands as a heuristic argument in favor of the existence of a non-trivial saddle point of a functional. There is however a major flaw in this reasoning – in some cases the quasilinear parabolic equations yield singularities in finite time. Actually in the particular case of the maps between spheres one can prove using a theorem by Struwe (Theorem 5) that the solution to the heat flow will blow up for some finite $t$.

In this thesis we analyse possible asymptotic states and the mechanism of the blow-up produced by the heat flow for maps between $k$-dimensional spheres. As the existence of harmonic maps between spheres has been proved by Bizoń and Chmaj [1], and Corlette and Wald [2] we focus on dynamical aspects of the heat flow such as stability analysis and the blow-up.
We start by defining the Dirichlet Energy and stating some basic facts about the harmonic maps in general. Next, we present a symmetric ansatz to reduce the problem of maps between spheres to maps between $S^1$ and we proceed by analysing the resulting quasilinear parabolic partial differential equation in one dimension. The stability of harmonic maps is analysed in section 3.2 and the blow-up mechanism is described in section 3.3.
Numerical results on solving the heat flow in the given ansatz are presented in chapter 4 to confirm the analytical results.

# Chapter 2

# Preliminaries

## 2.1 Harmonic maps

Given two manifolds $(M, g)$ and $(N, h)$ we define a smooth map $F : M \to N$. To comply with the terminology used in literature, from now on we will call $M$ the domain manifold and $N$ the target manifold. We shall construct the simplest possible scalar, which involves the metric tensors of both $(M, g)$ and $(N, h)$ and the mapping $F$.
Given the basis $e^i$ on $T_xM$, the simplest scalar function on $T_xM \otimes T_xM$ is the scalar product $<, >_x$ defined as

$$\langle e^i \otimes e^j, e^k \otimes e^l \rangle_x = g^{ik} g^{jl}. \tag{2.1}$$

For two tensors $\tau$ and $\tau'$ from $T_xM \otimes T_xM$ we then have

$$\langle \tau, \tau' \rangle_x = \tau^{ij} \tau'_{ij}. \tag{2.2}$$

Given the map $F$, we can construct the pullback $F^*h \in T_xM \otimes T_xM$ and use the above scalar product to contract $g$ and $F^*h$ and therefore build up a scalar function we intended

$$e(F) := \frac{1}{2} \langle g, F^*h \rangle_x. \tag{2.3}$$

This is the generalization of the Dirichlet energy density $\frac{1}{2}\|\nabla u\|^2$ for functions $u : M \to \mathbb{R}$, indeed, for real function $u$ we have

$$e(u) = \frac{1}{2} \langle g, u^* 1 \rangle = \frac{1}{2} g^{ij} \partial_i u \partial_j u = \frac{1}{2} \|\nabla u\|^2. \tag{2.4}$$

**Definition 1.** *We say that a map $F$ is regular if the corresponding Dirichlet energy density is finite*

$$e(F) < \infty. \tag{2.5}$$

Integrating $e(F)$ over $M$, we obtain the Dirichlet energy of the mapping $F$

$$E(F) = \int_M e(F) dV_M. \tag{2.6}$$

By defining a functional on the space of maps $M \to N$ we distinguish a class of maps for which the functional is extremalized. Depending on the domain manifold, the extrema of (2.6) have different names in literature: harmonic maps if the domain is Riemannian manifold, or wave maps if the domain is a Lorentzian manifold.

**Remark 1.** *Dirichlet energy of any map from a Riemannian manifold to a Riemannian manifold is non-negative.*

Using local coordinate charts $x^a$ on $M$ and $F^A$ on $N$ we can write (2.6) as

$$E(F) = \frac{1}{2} \int_M h_{AB}(F) \frac{\partial F^A}{\partial x^a} \frac{\partial F^B}{\partial x^b} g^{ab} dV_M. \tag{2.7}$$

It is convenient to introduce the so called tension field

$$\tau(F)^C = \Delta_g F^C + \Gamma^C_{AB}(h) \frac{\partial F^A}{\partial x^a} \frac{\partial F^B}{\partial x^b} g^{ab}, \tag{2.8}$$

where $\Delta_g$ is the Laplace-Beltrami operator on $M$ and $\Gamma^C_{AB}(h)$ is the Christoffel symbol of the Levi-Civita connection on $N$. The set of partial differential equations which the critical points of (2.7) has to satisfy can then be stated as

$$\tau(F)^C = 0. \tag{2.9}$$

From now on we shall assume that both the domain and the target manifolds are Riemannian and in consequence the above set of semi-linear partial differential equations is elliptic.

The problem of existence of nontrivial solutions to (2.9) in general is still open, but there is a variety of partial results starting from the classical theorem:

**Theorem 1** (Eells-Sampson [3]). *If $N$ is compact and has non-positive sectional Riemannian curvature, then every homotopy class of maps $M \to N$ contains a harmonic map whose energy is an absolute minimum in the given homotopy class.*

**Remark 2.** *One can also easily verify that the identity map $id : M \to M$ is a harmonic map, regardless of the choice of $M$, by substituting $F^A = x^A$ into (2.9). The energy density of the identity map is $e(id) = \dim(M)/2$.*

The following remark can be also proved easily.

**Remark 3.** *Given two harmonic maps $F_1 : M_1 \to N_1$ and $F_2 : M_2 \to N_2$, the map $F : M_1 \times M_2 \to N_1 \times N_2$ of the form $F((x_1, x_2)) = (F_1(x_1), F_2(x_2))$ is also harmonic.*

After this very brief introduction to harmonic maps we proceed to the problem to which this thesis is devoted.

## 2.2 Harmonic maps for $F : S^k \to S^k$

### General properties

From now on we shall set both the domain and target manifolds to $S^k$. We choose the coordinates on the domain sphere as

$$x^a = (\psi, \theta), \tag{2.10}$$

where $\psi \in (0, \pi)$ is the longitudal angle with south pole at $\psi = 0$ and $\theta$ is the set of coordinates on $S^{k-1}$ – the equator of $S^k$. Analogously we introduce coordinates $(\Psi, \Theta)$ on the target sphere in which the map $F$ takes the form

$$F^A(\psi, \theta) = (\Psi, \Theta). \tag{2.11}$$

The metric tensors for the given coordinate frames are

$$\text{domain:} \qquad ds^2 = d\psi^2 + \sin^2\psi ds^2\big|_{S^{k-1}} \tag{2.12}$$

$$\text{target:} \qquad dS^2 = d\Psi^2 + \sin^2\Psi dS^2\big|_{S^{k-1}}. \tag{2.13}$$

Solving equations (2.9) without any further assumptions presents an impossible task, therefore in section 2.2 we introduce a simple symmetric ansatz. Still without any simplifications we can state the following.

**Theorem 2.** *For $k \geq 3$ and any map $F : S^k \to S^k$ there is a map within the same homotopy class of arbitrary small Dirichlet energy.*

*Proof.* The proof is based on the fact that on a sphere there exists a one parameter group of conformal maps, which in the coordinates (2.10) have the form

$$\psi_A = 2\arctan(e^A \tan(\psi/2)). \tag{2.14}$$

The above conformal map can be depicted as dragging the whole sphere along the longitudal coordinates in the direction of one of its poles (for $A$ large, this would be the north pole). We define the map $F_A$ to be the composition

$$F_A = F \circ \psi_A. \tag{2.15}$$

As $\psi_A$ leaves the points $\psi = 0$ and $\psi = \pi$ unchanged, $F_A$ has the same homotopy degree as $F$. Due to the conformal properties of the map $\psi_A$ we obtain the following energy density of $F_A$

$$e(F_A)_\psi = e(F)_{\psi_A}\rho_A^2, \quad \rho_A = \frac{1}{\cosh A - \cos\psi \sinh A}, \tag{2.16}$$

where $e(F)_\psi$ is the energy density of $F$ at point $\psi$. The map $F$ is regular, hence $e(F)_{\psi_A}$ is bounded by its maximal value $C(F) = \max_\psi (e(F)_\psi)$, therefore

$$e(F_A)_\psi \leq C(F)\rho_A^2. \tag{2.17}$$

Assuming $k \geq 3$, the Dirichlet energy of $F_A$ can be bounded by

$$\begin{aligned} E(F_A) &= \int_{S^k} e(F_A) dV_{S^k} \\ &\leq C(F)V(S^{k-1}) \int_0^\pi \rho_A^2 \sin^{k-1}\psi d\psi \\ &\leq C(F)V(S^{k-1}) \max_\psi(\sin^{k-3}\psi) \int_0^\pi \rho_A^2 \sin^2 \psi d\psi \\ &\leq C_1(F,k)\frac{1}{1+\cosh A}, \end{aligned} \tag{2.18}$$

which can be made arbitrary small by choice of sufficiently large $|A|$.

□

### Harmonic map ansatz

We simplify our problem by assuming that $\Theta = \theta$ and $\Psi = f(\psi)$ so the map $F$ takes the form

$$F : (\psi, \theta) \to (f(\psi), \theta), \tag{2.19}$$

which leaves us with one function as a degree of freedom. The given setup has been introduced in [3] and it is based on an idea that, after removing the poles, $S^k$ can be treated as $(0, \pi) \times S^{k-1}$, for which we can use remarks 2 and 3 with $F_1 = f$ and $F_2 = \mathrm{id}$.

For $F$ to be continuous, we require that

$$\lim_{\psi\to 0} f(\psi) = n\pi, \quad \lim_{\psi\to\pi} f(\psi) = m\pi. \tag{2.20}$$

Moreover, closing the domain of $\psi$ will not have any implications as long as $F$ is regular so we can drop the limits from (2.20)

$$f(0) = n\pi \quad f(\pi) = m\pi. \tag{2.21}$$

The number $n - m$ stands for the homotopy degree of a map.

The Dirichlet energy of the considered map has now a more transparent form

$$E(f) = \frac{1}{2}\int_0^\pi \left(f'^2 + (k-1)\frac{\sin^2 f}{\sin^2\psi}\right)\sin^{k-1}\psi d\psi, \tag{2.22}$$

where we changed the argument of $E$ from $F$ to $f$ as effectively it is a functional of $f$ and we dropped the volume term $V(S^{k-1})$ which has no qualitative impact on the behaviour of the system. By the definition 1, the map $f$ is regular if

$$e(f) = \frac{1}{2}\left(f'^2 + (k-1)\frac{\sin^2 f}{\sin^2\psi}\right) < \infty. \tag{2.23}$$

Critical points of $E(f)$ are solutions to the corresponding Euler-Lagrange equation

$$\frac{1}{\sin^{k-1}\psi}\left(\sin^{k-1}\psi f'\right)' - \frac{(k-1)}{2}\frac{\sin 2f}{\sin^2\psi} = 0. \tag{2.24}$$

with the boundary values

$$f(0) = n\pi, \quad f(\pi) = m\pi. \tag{2.25}$$

The equation (2.24) has trivial solutions $f = n\pi$ of homotopy degree zero for which $E(f)$ attains absolute minimum: $E(n\pi) = 0$. By remark 2, the identity map $f = \psi + n\pi$ is also the solution but of the homotopy degree one. Hereafter we set $n = 0$ without loss of generality. By the nontrivial $\mathbb{Z}_2$ symmetry (the antipodal reflection)

$$f \to \bar{f} = \pi - f, \quad E(f) \qquad \to E(\bar{f}) = E(f), \tag{2.26}$$

every possible critical point will have its partner of the same homotopy degree. This is true unless $f$ is invariant under (2.26), but the only such case is $f_e = \pi/2$ which is not continuous thus not harmonic. (TODO: it does however play an important role and is described in grater detail in appendix). To be consistent with [1] we shall denote the constant and identity solutions as

$$f_0 = 0 \quad f_1 = \psi. \tag{2.27}$$

These, are the only solutions to (2.24) known in the closed form. More detailed analysis of (2.24) is contained in [1] and [2], where the infinite family of regular solutions for $3 \le k \le 6$ was found. Following the notation in [1], we denote the solutions as $f_n$, where $n \in \mathbb{N}_0$. The parametrization by $n$ is motivated by the property that $f_n$ has exactly $n$ intersections with $\pi/2$ and $n-1$ extrema. Each of $f_n$ is of homotopy degree zero for $n$ even or one for $n$ odd and stays inside the square $[0,\pi] \times [0,\pi]$. To be consistent with (2.27) we set $f_n(0) = 0$. The first few such harmonic maps are depicted in figure 2.1. From [1] it also follows that the solutions obey the following parity relation

$$f_n(\psi) = (-1)^n f_n(\pi - \psi). \tag{2.28}$$

In [2] the authors proved that $f_n$ has index $n$ (i.e. there are $n$ negative eigenvalues of the Hessian of the energy). From the last statement it follows that there are no local minima of $E(f)$ apart from $f_0$. As we will need the following property later on we introduce it as the theorem.

**Theorem 3** (Wald, Corlette [2])**.** *There are no local minima of $E(f)$ apart from $f = n\pi$.*

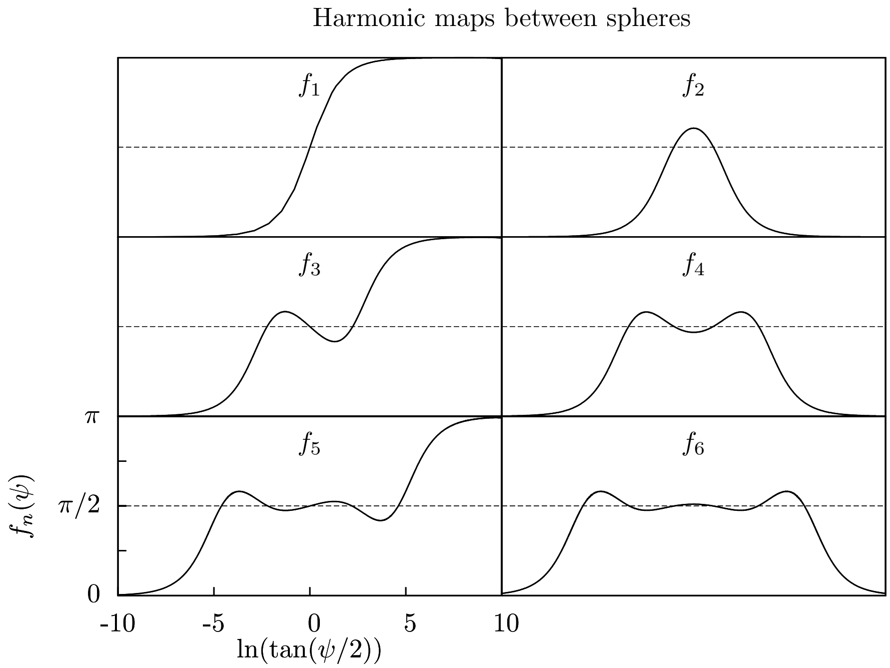


Figure 2.1: The first six non-trivial harmonic maps between spheres (solutions to (2.24)). $\ln(\tan(\psi/2))$ scale of the abscissa is due to the fact that each $f_n$ is steeper near the boundaries.

*Proof.* This can also be proved by showing that for each $n > 0$, $f_n$ there is at least one direction $v$ for which the Hessian is negative

$$\begin{aligned} \delta^2 E(f_n)(v,v) &= \int_0^\pi \left( v'^2 + (k-1)\frac{\cos 2f_n}{\sin^2\psi} v^2 \right) \sin^{k-1}\psi d\psi \\ &= (v, \mathcal{L}_n v), \end{aligned} \tag{2.29}$$

$$\mathcal{L}_n v = -\frac{1}{\sin^{k-1}\psi}\left(\sin^{k-1}\psi v'\right)' + (k-1)\frac{\cos 2f_n}{\sin^2\psi} v. \tag{2.30}$$

It turns out that the conformal Killing on $S^k$ field

$$K = \sin\psi \frac{\partial}{\partial\psi} \tag{2.31}$$

related to (2.14) generates such $v$, namely for $v = \sin\psi f_n'(\psi)$ by (A.2) we have

$$\mathcal{L}_n v = (2-k)v \tag{2.32}$$

$$\delta^2 E(f_n)(v,v) = (v, \mathcal{L}_n v) = (2-k)\|v\|^2 < 0. \tag{2.33}$$

This construction does not apply for $n = 0$ in which case $v = 0$. □

# Chapter 3

# Gradient flow

## 3.1 Heat flow

We can approach the problem of existence and the properties of critical points of a functional in several ways. For example in one dimensional case one can prove the existence of solutions to Euler-Lagrange equations using some ODE techniques, but this rarely gives insight into the geometry underlying the functional. Another more sophisticated way is to analyse the level sets of the functional and use the infinite dimensional variant of the Morse theory to obtain critical points as it has been done e.g. in [2]. Finally, there is a powerful technique called the heat flow, which consists of defining the flow, which moves along the gradient lines of the functional in the direction of the negative gradient.

The intuition behind the heat flow is that, if it exists for all times, it will push the solution into a minimum of the functional (if the functional is bounded from below). This approach is especially useful in finding a harmonic map of a given degree, because the degree is conserved during the flow.
The formal setup for the heat flow of the Dirichlet energy (2.7) is

$$\begin{aligned} &\partial_t F^A = -\delta E(F^A) = \tau(F)^A, \\ &F\big|_{t=0} = F_0 \end{aligned} \tag{3.1}$$

where

$$\tau(F)^C = \Delta_g F^C + \Gamma^C_{AB}(h)\frac{\partial F^A}{\partial x^a}\frac{\partial F^B}{\partial x^b}g^{ab}. \tag{3.2}$$

By our assumption on the domain and the target, (3.1) is the set of quasi-linear parabolic PDE's. Using (3.1) we get

$$\frac{dE}{dt} = -\int_M \partial_t F_A \partial_t F_B h^{AB} dV_M \leq 0 \tag{3.3}$$

with $dE/dt = 0$ if and only if $F$ is harmonic. The flow (3.1) therefore reduces the energy and asymptotically tends to a critical point of $E$.

The question if there exists a harmonic map in the same homotopy class as the initial data $F_0$ is thus reduced to the question of existence of a solution of (3.1) for all $t$ which is non singular as $t \to \infty$. This method was used in [3] to prove Theorem 1, which now can be reformulated in the following form:

**Theorem 4** (Eells-Sampson [3])**.** *If $N$ is compact and has non-positive sectional Riemannian curvature, then for every $F_0$ the solution to* (3.1) *exists for all times and converges to the minimizing harmonic map as $t \to \infty$.*

Unfortunately the technique of heat flow is not always so successful – the solutions to (3.1) are not guaranteed to exist for arbitrary large times. Actually, there is criterion which guarantees that the solution will cease to exist at some time $T$:

**Theorem 5** (Struwe [8])**.** *For any time $T > 0$ there exists a constant $\epsilon = \epsilon(T) > 0$ such that for any map $F_0 : M \to N$ which is not homotopic to a constant and satisfies $E(F_0) < \epsilon$ the solution $F$ to* (3.1) *must blow up before time $2T$.*

In the case when $M$ has non-positive Riemannian curvature the theorem is still true but empty, because within a given homotopy class, the smooth harmonic map attains the global minimum which is greater than the constant $\epsilon(T)$, thus no initial data can fulfill the criterion $E(F_0) < \epsilon$.

## Heat flow for $S^k \to S^k$

From this point we will assume that the map $F : S^k \to S^k$ satisfies the ansatz (2.19) and we shall consider the functional $E(f)$ as defined in (2.22) as a base for (3.1). Applying the heat flow to (2.22) we obtain the following initial boundary problem

$$\begin{aligned} f_t &= \frac{1}{\sin^{k-1}\psi}\left(\sin^{k-1}\psi f'\right)' - \frac{(k-1)}{2}\frac{\sin 2f}{\sin^2\psi}, \\ f(0,\psi) &= g(\psi), \\ f(t,0) &= g(0) = 0 \quad f(t,\pi) = g(\pi) = m\pi. \end{aligned} \tag{3.4}$$

The integer $m$ is equal to the topological degree of the map. By (3.3) the energy decreases

$$\frac{dE}{dt} = -\int_0^\pi f_t^2 \sin^{k-1}\psi d\psi < 0 \tag{3.5}$$

unless $f$ is a stationary point of $E(f)$. By Theorem 3 the only point to which the flow can converge starting from generic initial data is the constant map

$f = n\pi$ for which the energy is zero. The flow will thus reduce the energy from $E(g)$ to an arbitrary small value. If the initial data is not homotopic to a constant, Theorem 5 comes into play, which combined with theorem 3 guarantees that the blow-up will occur. Moreover, by the numerical evidence, even if the boundary values are of the form $g(0) = g(\pi) = 0$ the blow-up can occur if initial data lie in the basin of attraction of $f = \pi$.

The flow (3.4) conserves the parity of $g$, namely if

$$g(\psi) = \pm g(\pi - \psi) \tag{3.6}$$

then at any given time $t \geq 0$ we have

$$f(t, \psi) = \pm f(t, \pi - \psi). \tag{3.7}$$

Our aim is to make the flow converge to one of the stationary points of $E$, which we know to have the parity specified by (2.28). We will henceforth denote by $g_+$ and $g_-$ initial data obeying

$$g_+(\psi) = g_+(\pi - \psi), \quad g_-(\psi) \qquad = -g_-(\pi - \psi) \tag{3.8}$$

which evolve in the subspaces $H_+$ and $H_-$ defined by

$$H_\pm = \{f(t, \psi)| \quad f(t, \psi) = \pm f(t, \pi - \psi)\}. \tag{3.9}$$

We also remark that

$$f_{2n} \in H_+, \quad f_{2n+1} \in H_-. \tag{3.10}$$

$f_0$ is the global energy minimizer in $H_+$ and $f_1$ is the global energy minimizer in $H_-$. The energy minimizing property of $f_0$ is a straightforward, the case of $f_1$ being the energy minimizer for $H_-$ is not that obvious but follows from the Morse analysis made in [2]. Generic initial data with suitable boundary conditions in any of those subspaces will converge to one of their respective ground states unless blow-up occurs. We will discuss the linear stability of the ground states $f_0$ and $f_1$ in the following section.

## 3.2 Stability of harmonic maps

As we know already, $f_0$ is the global minimum of the Dirichlet energy and we expect it to be linearly stable. Also $f_1$ should turn out to be linearly stable under antisymmetric perturbations, and unstable under the symmetric ones due to theorem 3 and (3.7). The linear stability can be approached by determining the eigenvalues of the Hessian $\delta^2 E(f_n)$ introduced in (2.29) which corresponds to solving the eigenproblem

$$\mathcal{L}_n v = \lambda v, \tag{3.11}$$
$$\mathcal{L}_n v = -\frac{1}{\sin^{k-1}\psi}\left(\sin^{k-1}\psi v'\right)' + (k-1)\frac{\cos 2f_n}{\sin^2\psi}v. \tag{3.12}$$

The Hilbert space for this problem is $\mathcal{H} = L^2([0,\pi], \sin^{k-1}\psi d\psi)$. If we perturb $f_n$ in the direction of $v$, the perturbed state will evolve as

$$f = f_n + e^{-\lambda t}v \tag{3.13}$$

which follows from linearizing (3.4) around $f_n$.

By $f_n(0) = 0$, the equation (3.11) near $\psi = 0$ takes the form

$$v'' + \frac{k-1}{\psi}v' - \frac{k-1}{\psi^2}v = 0. \tag{3.14}$$

We obtain the indicial equation by substituting $v(\psi) = \psi^\gamma$ obtaining

$$\gamma(\gamma-1) + (k-1)\gamma - (k-1) = 0 \tag{3.15}$$

with the solutions

$$\gamma = 1 \quad \text{or} \quad \gamma = 1-k, \tag{3.16}$$

of which only the first one corresponds to $v \in \mathcal{H}$. The analogous asymptotic behaviour can be derived at $\psi = \pi$ where also only one solution is in $\mathcal{H}$. We will denote the $m$-th eigenvalue of $\mathcal{L}_n$ as $\lambda_m^{(n)}$ and the associated eigenvectors as $v_m^{(n)}$ with $m \in \mathbb{N}_0$. The eigenvalues are ordered as follows

$$\lambda_0^{(n)} < \lambda_1^{(n)} < \lambda_2^{(n)} < \dots \quad . \tag{3.17}$$

From the fact that $\mathcal{L}_n$ is symmetric under $\psi \to \pi - \psi$ (by (2.28)), it follows that $v$ can be either symmetric or antisymmetric. We can use the Sturm oscillation theorem [7] to determine the exact parity of eigenvectors by the fact that $v_m^{(n)}$ should have $m-1$ zeroes, from which it follows that

$$v_m^{(n)}(\psi) = (-1)^m v_m^{(n)}(\pi - \psi). \tag{3.18}$$

As mentioned in the proof of theorem 3, for $n \geq 1$ each $f_n$ has the eigenvector generated by the conformal Killing field and defined as follows

$$v_{\text{conf}}^{(n)} = \sin\psi f_n'(\psi), \tag{3.19}$$

corresponding to the $\lambda_{\text{conf}}^n = (2-k)$. As $f_n'(\psi)$ has exactly $n-1$ zeroes, there are $n-1$ eigenvalues smaller than $\lambda_{\text{conf}}^n = (2-k)$ which follows from the Sturm oscillation theorem. We shall therefore denote

$$v_{n-1}^{(n)} = \sin\psi f_n'(\psi) \quad \lambda_{n-1}^{(n)} = (2-k). \tag{3.20}$$

### Stability of $f_0$

By (3.11)(3.12), the eigenproblem for $f_0$ is

$$\mathcal{L}_0 v = \lambda v, \tag{3.21}$$

$$\mathcal{L}_0 v = -\frac{1}{\sin^{k-1}\psi}\left(\sin^{k-1}\psi v'\right)' + \frac{(k-1)}{\sin^2\psi} v. \tag{3.22}$$

We can multiply (3.11) by $v \sin^{k-1}\psi$ and integrate on the interval $[0,\pi]$ to get

$$\lambda \int_0^\pi v^2 w d\psi = \int_0^\pi \left(v'^2 + \frac{k-1}{\sin^2\psi} v^2\right) \sin^{k-1} d\psi > 0. \tag{3.23}$$

All the terms under the integrals are positive for $v \neq 0$ so $\lambda > 0$ and $f_0$ is linearly stable. We can calculate the spectrum of (3.22) explicitly. First we change the independent function to

$$w(\psi) = v(\psi) \sin^{(k-1)/2}\psi \tag{3.24}$$

and the eigenproblem (3.21) simplifies to

$$-w'' + V_0(\psi) w = \left(\lambda - \frac{1}{2}(k-1)\right) w, \tag{3.25}$$

$$V_0(\psi) = \frac{1}{4}(k^2-1)\cot^2\psi. \tag{3.26}$$

The solution to (3.25) with the proper asymptotic at $\psi = 0$ can be written in terms of the associated Legendre polynomials

$$w(\psi) = \sqrt{\sin\psi} P_\beta^{-\alpha}(\cos(\psi)), \tag{3.27}$$

$$\alpha = \frac{k}{2}, \quad \beta = -\frac{1}{2} + \frac{1}{2}\sqrt{(k-1)^2 + 4\lambda}. \tag{3.28}$$

We now analyse the behaviour at $\psi = \pi$ by expanding $P_\beta^{-\alpha}$ around $\cos\pi = -1$

$$\begin{aligned} &P_\beta^{-\alpha}(z) = \\ &\frac{2^{\alpha/2}\Gamma(\alpha)}{\Gamma(\alpha-\beta)\Gamma(\beta+\alpha+1)}(z+1)^{-\alpha/2}(1+\mathcal{O}((z+1))) \\ &-\frac{1}{\pi}2^{-\alpha/2}\sin(\pi\beta)\Gamma(-\alpha)(1+z)^{\alpha/2}(1+\mathcal{O}((z+1))) \end{aligned} \tag{3.29}$$

The quantization of $\lambda$ is obtained by setting the coefficient in the first term to zero. This can be achieved only by selecting $\beta$ so that one of the functions $1/\Gamma(z)$ will be zero, which implies $\beta \in \mathbb{R}$. But then $\beta + \alpha + 1 > 0$ and the only possible zeroes are for

$$\alpha - \beta = -m, \quad m \in \mathbb{N}_0 \tag{3.30}$$

which gives rise to the following quantization of $\lambda$

$$\lambda_m^{(0)} = (1+m)(k+m). \tag{3.31}$$

The eigenvectors corresponding to (2.22) are

$$w_0^{(m)}(\psi) = \sqrt{\sin\psi}\,P_{k/2+m}^{-k/2}(\cos\psi). \tag{3.32}$$

By the parity properties of $P_{k/2+m}^{-k/2}$ we get the symmetric and antisymmetric families of eigenvectors

$$w_0^{(m)}(\psi) = (-1)^m w_m^0(\pi-\psi) \tag{3.33}$$

which agrees with (3.18). Going back to the eigenvectors of $\mathcal{L}_0$ we obtain

$$v_0^{(m)}(\psi) = \sin(\psi) C_m^{\left(\frac{1+k}{2}\right)}(\cos\psi), \tag{3.34}$$

where $C_m^{(\lambda)}$ are the Gegenbauer polynomials connected to the Legendre polynomials [6] by

$$P_\nu^\mu(x) = \frac{2^\mu\,\Gamma(1-2\mu)\,\Gamma(\nu+\mu+1)}{\Gamma(\nu-\mu+1)\,\Gamma(1-\mu)\,(1-x^2)^{\mu/2}}\,C_{\nu+\mu}^{(\frac{1}{2}-\mu)}(x)\,. \tag{3.35}$$

The relation to Gegenbauer polynomial was emphasized because $C_m^{(\delta)}(x)$ are polynomials in $x$ of degree $m$. The closed form of $v_m^{(0)}$ for first few $m$ are given below.

$$\begin{aligned}
v_0^{(0)} &= \sin(\psi),\\
v_1^{(0)} &= \frac{1}{2}(k+1)\sin(2\psi),\\
v_2^{(0)} &= \frac{1}{8}\left(k^2-1\right)\sin(\psi) + \frac{1}{8}\left(k^2+4k+3\right)\sin(3\psi),\\
v_3^{(0)} &= \frac{1}{48}\left(2k^3+6k^2-2k-6\right)\sin(2\psi) + \frac{1}{48}\left(k^3+9k^2+23k+15\right)\sin(4\psi).
\end{aligned} \tag{3.36}$$

### Stability of $f_1$

For $f_1$ the eigenproblem is stated as

$$\mathcal{L}_1 v = \lambda v. \tag{3.37}$$

$$\mathcal{L}_1 v = -\frac{1}{\sin^{k-1}\psi}\left(\sin^{k-1}\psi v'\right)' + (k-1)\frac{\cos 2\psi}{\sin^2\psi}v \tag{3.38}$$

We can get the bound similar to (3.23) but valid only for the antisymmetric eigenvectors (otherwise the boundary terms from the integration by parts do not vanish) by integrating (3.37) on the interval $[0,\pi/2]$

$$\lambda\int_0^{\pi/2} v^2 w d\psi = \int_0^{\pi/2}\left(v'^2 + (k-1)\frac{\cos 2\psi}{\sin^2\psi}v^2\right)\sin^{k-1} d\psi > 0. \tag{3.39}$$

(3.37) is also solvable by the procedure similar to that used in the case of $f_0$ which yields

$$v_1^{(m)}(\psi) = \sin(\psi) C_m^{\left(\frac{1+k}{2}\right)}(\cos\psi), \tag{3.40}$$

$$\lambda_m^{(1)} = 2 + k(-1+m) + m + m^2. \tag{3.41}$$

The only eigenvalue smaller than zero is $\lambda_0^{(1)} = 2 - k$ and, by $C_0^{(\delta)}(x) = 1$, the corresponding eigenvector is $v_1^{(0)} = \sin\psi$. By (3.34), $v_m^{(0)} = v_m^{(1)}$ so the table (3.36) gives the closed forms of $v_m^{(1)}$.

### Stability of $f_2$ and $f_3$

Although we cannot solve (3.11) analytically for $n \geq 2$ we know the number of negative eigenvalues from theorem 3 and the parity of the corresponding eigenvectors from (3.18). We use that knowledge to reduce the number of unstable directions by restricting the possible perturbations to those belonging to $H_+$ or $H_-$. By this procedure we kill all the antisymmetric modes of $\mathcal{L}_2$ and the symmetric ones of $\mathcal{L}_3$ reducing the number of instabilities of $f_2$ and $f_3$ to one. We can thus write the perturbed solutions around $f_2$ and $f_3$ as

$$f_+ = f_2 + A_0 e^{-\lambda_0^{(2)} t} v_2^{(0)} + A_2 e^{-\lambda_2^{(2)} t} v_2^{(2)} + \dots, \tag{3.42}$$

$$f_- = f_3 + B_1 e^{-\lambda_1^{(3)} t} v_3^{(1)} + B_3 e^{-\lambda_3^{(3)} t} v_3^{(3)} + \dots. \tag{3.43}$$

The first modes are unstable while the latter are stable. This will be used in the following sections where we shall determine the first two modes of $f_{2,3}$ by solving the PDE (3.4) numerically.

## 3.3 Blow-up

Although the theorem 5 states that some kind of singular behaviour will occur, it does not tell us what is the form of blow-up. We shall now turn onto the mechanism of blow-up for the gradient flow of the maps $S^k \to S^k$.

From now on we assume that the blow-up time $T$ is known a priori. By symmetry, the blow-up can be localized only on the edges of the interval $[0, \pi]$. Because of the reflection symmetry $f(\psi) \to f(\pi - \psi)$ of the gradient flow equations we can focus our analysis at one of the edges, say $\psi = 0$. Because the blow-up is localized within some small neighbourhood of a pole of $S^k$, the curvature of the domain does not play any role so we change the domain manifold to $\mathbb{R}^k$ being the space tangent to $S^k$ at $\psi = 0$. Therefore in this section we will analyse the behaviour of the gradient flow for maps $\mathbb{R}^k \to S^k$ satisfying the ansatz analogous to (2.19) but with the metric tensors of the domain and the target manifolds given by

$$\text{domain:} \qquad ds^2 = dr^2 + r^2 ds^2\big|_{S^{k-1}} \tag{3.44}$$

$$\text{target:} \qquad dS^2 = dh(r)^2 + \sin^2 h(r) dS^2\big|_{S^{k-1}}. \tag{3.45}$$

The role of $\psi$ is then taken by the radial variable $r$ and $f$ is replaced by $h$. The Dirichlet energy of $h$ is

$$E(h) = \frac{1}{2}\int_0^\infty \left(h'^2 + (k-1)\frac{\sin^2 h}{r^2}\right) r^{k-1} dr, \tag{3.46}$$

from which the following tension field can be derived

$$\tau(h) = h'' + \frac{(k-1)}{r}h' - \frac{k-1}{2}\frac{\sin 2h}{r^2}. \tag{3.47}$$

The Euler-Lagrange equations for the stationary point of $E(h)$ are

$$\tau(h) = 0, \quad h(0) = 0, \quad h(\infty) = m\pi. \tag{3.48}$$

The boundary condition at $\infty$ follows from the finiteness of $E(h)$. As in the case of the maps $S^k \to S^k$, (3.46) has no stable stationary points apart from $n\pi$. This can be shown using the conformal transformation $r_A : \mathbb{R}^k \to \mathbb{R}^k$ and the rescaled function $h_A$ defined as follows

$$r_A(r) = e^A r, \quad h_A = h \circ r_A. \tag{3.49}$$

The energy of $h_A$ is

$$E(h_A) = e^{(2-k)A}E(h) \tag{3.50}$$

and therefore for any $h \neq n\pi$ the energy can be decreased by rescaling the domain manifold. Also the tension field scales as follows

$$\tau(h_A)_r = e^{2A}\tau(h)_{r_A} \tag{3.51}$$

where $\tau(h)_r$ is the tension field at the point $r$. The gradient flow for $E(h)$ is defined as

$$\partial_t h = \tau(h), \quad h(0) = 0, \quad h(\infty) = m\pi. \tag{3.52}$$

The simple scaling property of the tension field motivates the ansatz

$$h(t, r) = H(e^{A(t)}r). \tag{3.53}$$

The idea behind such ansatz is that the solutions to (3.52) could consist of a constant profile sliding along the path generated by the conformal transform. Substituting (3.53) to (3.52) gives us

$$A'(t)e^{-2A(t)}yH'(y) = \tau(H)_y. \tag{3.54}$$

$H$ is the function of $y$ only, so the term involving $t$ has to be constant and we get

$$A'(t)e^{-2A(t)} = C, \tag{3.55}$$

$$e^{2A} = \frac{1}{\sqrt{2C(T-t)}}, \tag{3.56}$$

$$CyH(y) = \tau(H)_y. \tag{3.57}$$

The choice of the sign of $C$ corresponds to the choice between the solutions which expand or shrink in time. The possibly singular behaviour is displayed only by the function which shrinks in time because if $H$ solves (3.57) its first spatial derivative at $r = 0$ is

$$\partial_r \left[H(y)\right]_{r=0} = \frac{1}{\sqrt{2C(T-t)}} H'(0). \tag{3.58}$$

From (3.57), by the equation similar to (3.15), we know that the only possible asymptotic behaviour of $H$ at $y = 0$ fulfilling $H(0) = 0$ is $H \sim y$, therefore $H'(0) \neq 0$. We conclude that for $C > 0$ the quantity (3.58) blows up in time $T$. In the literature this type of singularity is called the type I blow-up. We can fix $C$ to $1/2$ by setting the argument of $H$ to

$$y = \frac{r}{\sqrt{T-t}}, \tag{3.59}$$

$$\frac{1}{2} y H'(y) = \tau(H)_y. \tag{3.60}$$

By the fact that the solution to (3.60) has to be regular for any $r > 0$ and any time $t$ including $t = T$ we have to impose the condition on $H$

$$\forall r > 0 : \lim_{t \to T} \left| H\left(\frac{r}{\sqrt{T-t}}\right)\right| = |H(\infty)| < \infty. \tag{3.61}$$

Such requirement, together with $0 = f(t, 0) = H(0)$, gives us the proper boundary conditions for possible static solutions to (3.65). We are therefore looking for the solutions to the ODE

$$\begin{aligned} &H'' + \left(\frac{(k-1)}{y} - \frac{y}{2}\right) H' - \frac{k-1}{2}\frac{\sin 2H}{y^2} = 0, \\ &H(0) = 0, \quad H'(\infty) = 0. \end{aligned} \tag{3.62}$$

There is also another approach to obtain (3.62) called a self-similar ansatz. It consist of setting $h = H(y)$ with $y$ as in (3.59) a priori to solving (3.55). It took its name from the fact that such ansatz is invariant under the self-similar symmetry of (3.52) given by

$$r \to \lambda r, \quad (T-t) \to \lambda^2 (T-t). \tag{3.63}$$

The complete set of self-similar variables consists of $y$ and the logarithmic time $s$ defined by the relations

$$y = \frac{r}{\sqrt{T-t}}, \quad s = -\log(T-t), \quad h(t, r) = H(s, y). \tag{3.64}$$

In such variables (3.52) takes the form

$$\partial_s H = H'' + \left(\frac{(k-1)}{y} - \frac{y}{2}\right) H' - \frac{k-1}{2}\frac{\sin 2H}{y^2}. \tag{3.65}$$

The self-similar solution $H = H(y)$ is therefore a stationary point of (3.65).

Fan [4] used ODE techniques to prove the existence of the family of solutions to (3.62) $H_n$, $n \geq 0$, for $3 \leq k \leq 6$ with the structure similar to that of the harmonic maps between spheres. As in the case of $f_0$, there is the trivial solution $H_0 = 0$. Then, for $n \geq 1$ each $H_n$ has the nodal number $n$, $n-1$ extrema and $H_n \in [0, \pi]$. Also the index of $H_n$, albeit not known analytically, can be found numerically to be $n$.
The original equation possesses a translational symmetry in the time variable, this means that $H_n(r/\sqrt{T-t})$ is a solution to (3.52) for any choice of the blow-up time $T$. The ambiguity in the choice of $T$ manifests itself as a gauge mode. To obtain the explicit form of this mode we can ask what happens if the blow-up is realized by $H_n$, but it occurs at time $T'$ which is a bit different from $T$, say $T' = T + \delta$. In such situation we have

$$\begin{aligned} H_n\left(\frac{r}{\sqrt{T+\delta-t}}\right) &= H_n\left(\frac{r}{\sqrt{T-t}}\right) - \delta\frac{1}{2}\frac{r}{(T-t)^{3/2}}H_n'\left(\frac{r}{\sqrt{T-t}}\right) + \mathcal{O}(\delta^2) \\ &= H_n(y) - \frac{\delta}{2}e^s y H_n'(y) + \mathcal{O}(\delta^2) \end{aligned} \tag{3.66}$$

which means that the change of the blow-up time by $\delta$ results in the exponentially increasing perturbation along the mode $yH_n'$ with the associated eigenvalue $-1$. This means, that among $n$ unstable modes of $H_n$ there is one gauge mode and thus $H_1$ possesses no unstable modes apart from the gauge one and the blow-up can be realized by the profile of $H_1$.

## 3.4 Bisection

Although we already know that $f_2$ and $f_3$ are saddle points of $E(f)$ we shall demonstrate in this section how to obtain them using only the heat flow (3.4).

Let us formally denote the basins of attraction of 0 and $\pi$ as $\Gamma(0)$ and $\Gamma(\pi)$ respectively. We say formally, because the solutions to (3.4) will blow up (e.g. by Theorem 5) before asymptotically converging to either of the ground states. We start by choosing $g_+ \in \Gamma(\pi) \cap H_+$ and $g_+(0) = g_+(\pi) = 0$. We now form a path $g_A \in H_+$ such that

$$g_A = A \cdot g_+, \quad A \in [0, 1]. \tag{3.67}$$

Obviously for $0 \leq A \ll 1$, $g_A \in \Gamma(0)$, so the curve intersects both, $\Gamma(0)$ and $\Gamma(\pi)$. As $\Gamma(\pi)$ and $\Gamma(0)$ are disjoint open sets, the curve leading from one of them into another has to contain the closed set which does not belong to either of the open sets. By definition, initial data from this set cannot fall into any of those attractors. This means that there is at least one $A^*$ such that the flow starting from $g_{A^*}$ is not going to converge to the global energy minimum. Still, for any initial data the energy has to decrease along the flow and for $A = A^*$ it cannot asymptotically decrease to 0, so its infimum $E^*$ obeys

$$E^* = \inf_{t \geq 0} E(t) > 0 \tag{3.68}$$

and hence, if $g_{A^*}$ does not blow up, the limiting values are

$$\lim_{t\to\infty} E(t) = E^* > 0, \quad \lim_{t\to\infty} \frac{dE}{dt}(t) = 0. \tag{3.69}$$

But, $dE/dt \to 0$ can happen only if $\partial_t f \to 0$ so

$$\lim_{t\to\infty} f(t,\psi) = f^*(\psi) \tag{3.70}$$

which means, that $f^*$ is a symmetric solution to (2.24) with $E(f^*) = E^*$, different from the ground states and, by construction, it is a saddle point in $H_+$. As $g_+$ was chosen to be generic, by such procedure we will obtain the saddle point of the lowest index, namely $f^* = f_2$.

Analogous procedure can be applied to $H_-$ with $(\psi + g_-) \in H_- \cap \Gamma(\pi - \psi)$, $g_-(0) = g_-(\pi) = 0$ and

$$g_B = \psi + B \cdot g_-, \quad B \in [0,1] \tag{3.71}$$

to obtain $f_3$.

## Chapter 4

# Numerical results

### 4.1 Numerical realization of the bisection

The procedure described in 3.4 can be easily realized by solving the PDE (3.4) numerically. For $H_+$, we start by choosing $g_+$ to be

$$g_+(\psi) = \sin\psi. \tag{4.1}$$

Then, the proper $A^*$ is found by bisection between the blow-up and the convergence to 0. As the bisection cannot yield an exact value of $A^*$ (due to the finite machine precision) we are not able to reach precisely the saddle point. Rather, as we are starting a bit off the border between attractors, the solution slides along it reaching the neighbourhood of $f_2$ along its stable direction, it stays there for some time but then starts to move away, slowly decaying along the unstable direction to finally either fall into 0 or blow up. The smaller the numerical error of $A^*$ the closer we get to the border and the longer solutions stays near $f_2$.

From the numerical solutions to PDE (3.4) we can read off the quantities involved in approaching and leaving the neighbourhood of $f_2$. These are the first two modes of $f_2$ along with their respective eigenvalues as presented in (3.42). To obtain the eigenvalues $\lambda_{0,2}^{(2)}$ we use the function $\partial_t\partial_\psi f\big|_{\psi=0}$ which, while in a close neighbourhood of $f_2$ is

$$\partial_t\partial_\psi f\big|_{\psi=0} = C_0 e^{-\lambda_0^{(2)}t} + C_2 e^{-\lambda_2^{(2)}t}. \tag{4.2}$$

After obtaining the data points from numerically solving PDE (3.4), we fit (4.2) with $C_{0,2}$ and $\lambda_{0,2}^{(2)}$ as free parameters. $C_{0,2}$ depend on the normalization of the unknown functions $v_{0,2}$ and their numerical values are insignificant to us. The same relation can be used to determine $\lambda_{1,3}^{(3)}$ while close to $f_3$ by

$$\partial_t \partial_\psi f\big|_{\psi=0} = C_0 e^{-\lambda_1^{(3)} t} + C_2 e^{-\lambda_3^{(3)} t}, \tag{4.3}$$

and similarly for $f_{0,1}$

$$\partial_t \partial_\psi f\big|_{\psi=0} = D_0 e^{-\lambda_0^{(0)}} \tag{4.4}$$

$$\partial_t \partial_\psi f\big|_{\psi=0} = D_1 e^{-\lambda_0^{(1)}}. \tag{4.5}$$

The results from fitting to (4.2) and (4.3) compared to numerically solving (3.11) are shown in the table 4.1.

| $\lambda_m^{(n)}$ | Heat flow | Eigenproblem |
|---|---|---|
| $\lambda_0^{(0)}$ | 2.9670 | 3 |
| $\lambda_1^{(1)}$ | 3.9963 | 4 |
| $\lambda_0^{(2)}$ | -2.8924 | -2.8926 |
| $\lambda_2^{(2)}$ | 4.5899 | 4.5911 |
| $\lambda_1^{(3)}$ | -10.5946 | -10.6650 |
| $\lambda_3^{(3)}$ | 4.4004 | 4.3942 |

Table 4.1: Comparison of the eigenvalues calculated by solving (3.4) and by solving (3.11) for $k = 3$. The values from solving eigenproblem for $n = 0, 1$ are exact by (3.31) and (3.41).

## 4.2 Details of numerical calculations

Both, the eigenproblem and the heat flow have been simulated using the programs written in ANSI C and using double precision arithmetic. The GSL library provided the set of standard time marching procedures using Runge-Kutta algorithms [5].

ODE (2.24) have been solved by shooting from $(\psi, f) = (0, 0)$ to the saddle points $(\pi, 0)$ and $(\pi, \pi)$. Eigenproblem has been solved parallel to the ODE (2.24) and eigenvalues have been obtained by the shooting method as well. In both problems we have used the series approximation to start near $(0, 0)$ but not at $(0, 0)$, as $(0, 0)$ is a saddle point.

The PDE (3.1) have been solved using the methods of lines with the derivatives on r.h.s. of (3.1) approximated by the three point stencils (order 2 for the first derivative, order 1 for the second derivative). Stencils were symmetric inside the grid and asymmetric on both of its edges. The time marching was run by the Runge-Kutta-Fehlberg (4,5) method from the GSL library [5]. The details of the simulations giving rise to the figures 4.1–4.4 are given in table 4.2.

| | | |
|---|---|---|
| Grid points | 400 | 400 |
| Domain | $[0, \pi/2]$ | $[0, \pi]$ |
| Initial data | $\psi + B\sin(2\psi)$ | $A\sin(\psi)$ |
| Critical value | $B = 1.24571310318894035$ | $A = 2.10669393489537526$ |
| Bisection error | $B^* = B \pm 10^{-15}\%$ | $A^* = A \pm 10^{-15}\%$ |
| Stepping function | `rkf45` | `rkf45` |

Table 4.2: Detailed parameters of numerical simulations.

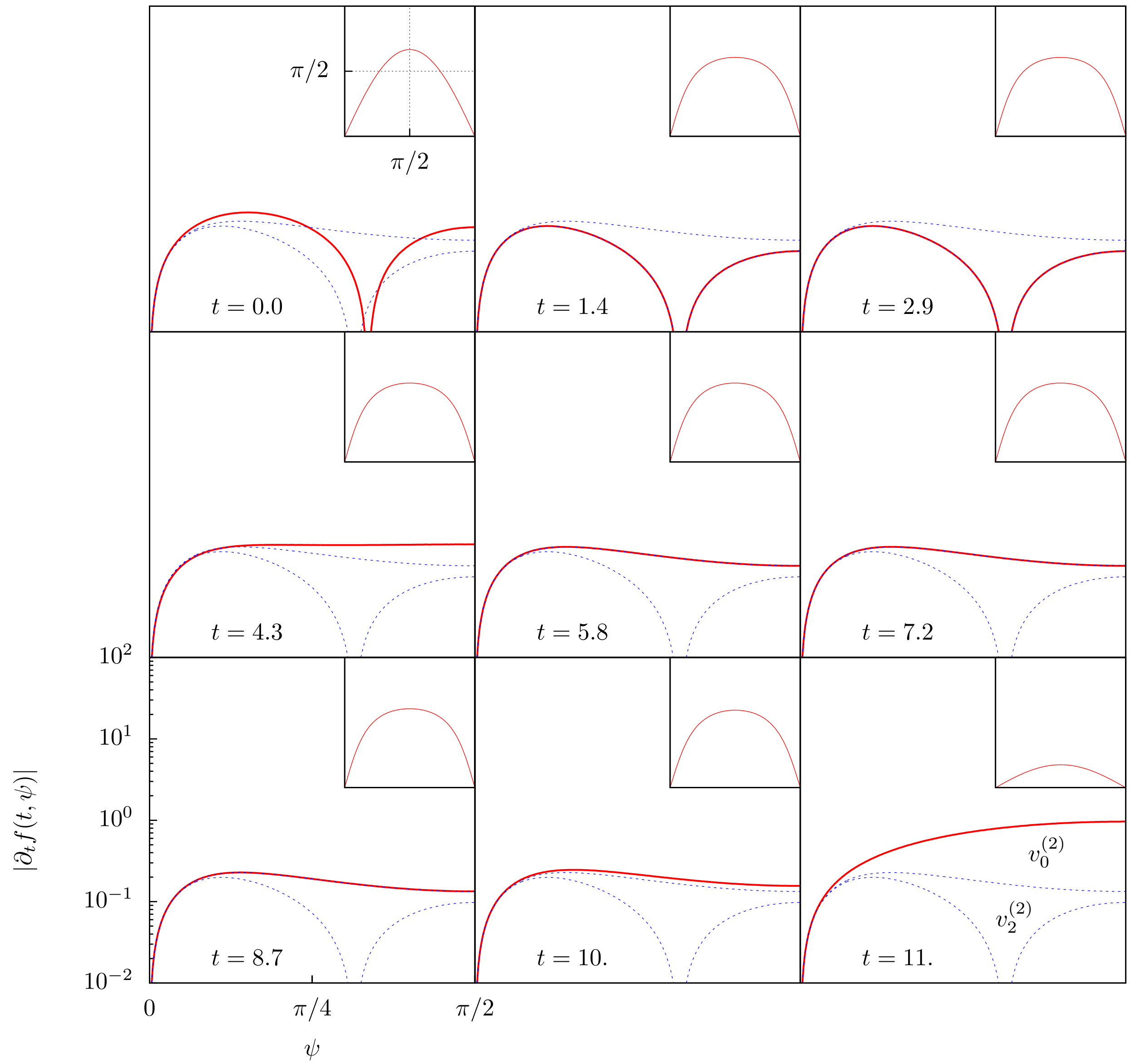


Figure 4.1: Sequence of snapshots of numerical solutions to the heat flow with initial data $g_+(\psi) = A \cdot \sin(\psi)$ with $A$ as in 4.2. Each snapshot depicts $|\partial_t f|$ (red line, larger plot) normalized so that $|\partial_t \partial_\psi f(t, 0)| = 1$ along with the plot of $f(t)$ (the plot in the upper right corner). For comparison the first two modes of $f_2$ (blue dashed lines), normalized to $v_{0,2}^{(2)\prime}(0) = 1$ have been also depicted. The evolution can now be divided into the following stages: ($t = 0.0$) non-linear approach to $f_2$, ($t = 1.4-2.9$) linear convergence to $f_2$ along $v_2^{(2)}$, ($t = 4.3-10.$) linear divergence along $v_0^{(2)}$, ($t = 3.5$) non-linear approach to ground state $f_0$, ($t \geq 4$) linear convergence to $f_1$ along $v_1^{(1)}$.

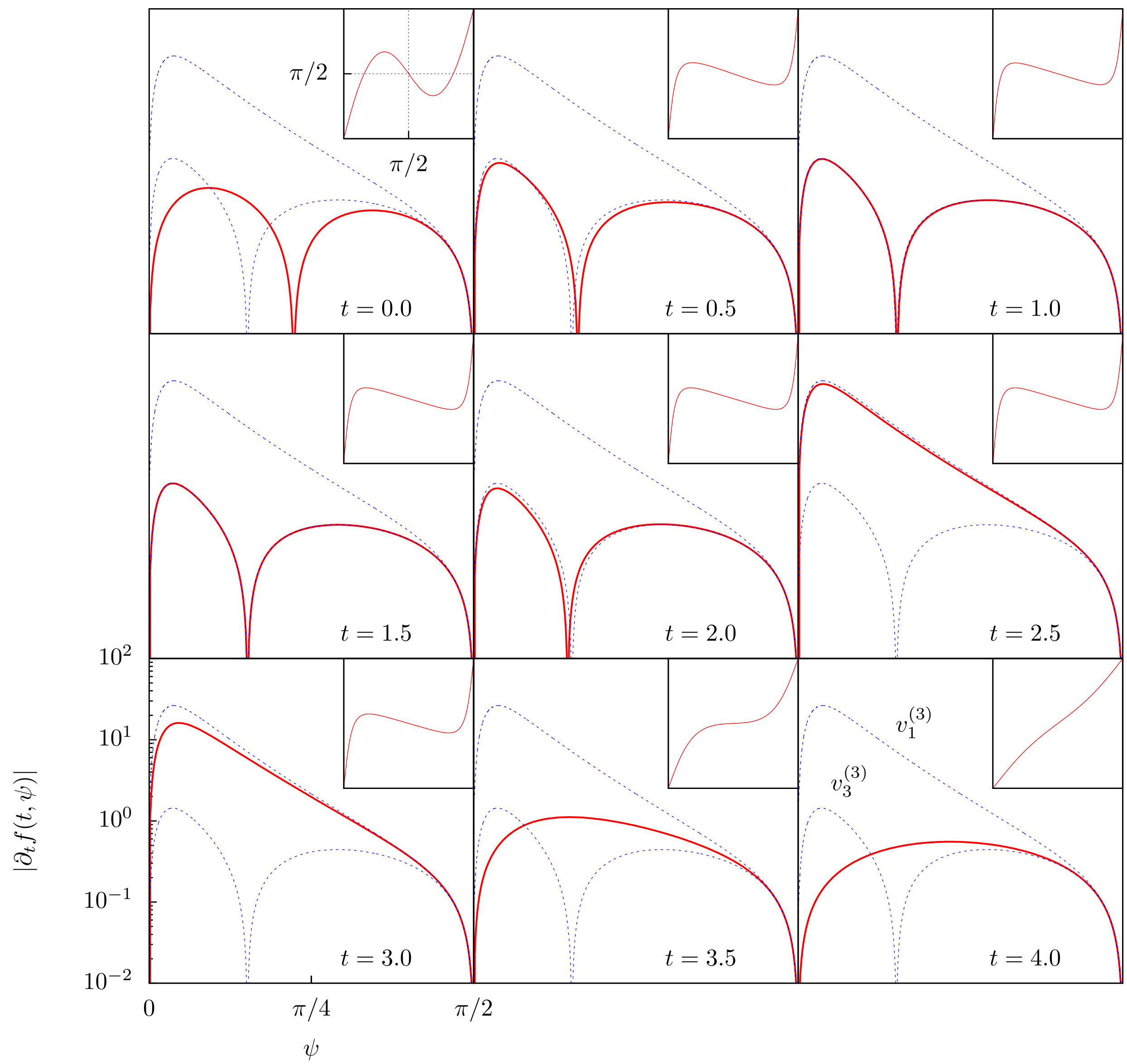


Figure 4.2: Sequence of snapshots of numerical solutions to the heat flow with initial data $g_-(\psi) = \psi + B \cdot \sin(2\psi)$ with $B$ as in 4.2. Each snapshot depicts $|\partial_t f|$ (red line, larger plot) normalized so that $|\partial_t \partial_\psi f(t, \pi/2)| = 1$ along with the plot of $f(t)$ (the plot in the upper right corner). For comparison the first two modes of $f_3$ (blue dashed lines), normalized to $v_{1,3}^{(3)\prime}(\pi/2) = 1$ have been also depicted. The evolution can now be divided into the following stages: $(t = 0)$ non-linear evolution, $(t = 1.5 - 2)$ linear convergence to $f_3$ along $v_3^{(3)}$, $(t = 2.5 - 3.)$ linear divergence along $v_1^{(3)}$, $(t = 3.5)$ non-linear approach to ground state $f_1$, $(t \geq 4)$ linear convergence to $f_1$ along $v_1^{(1)}$.

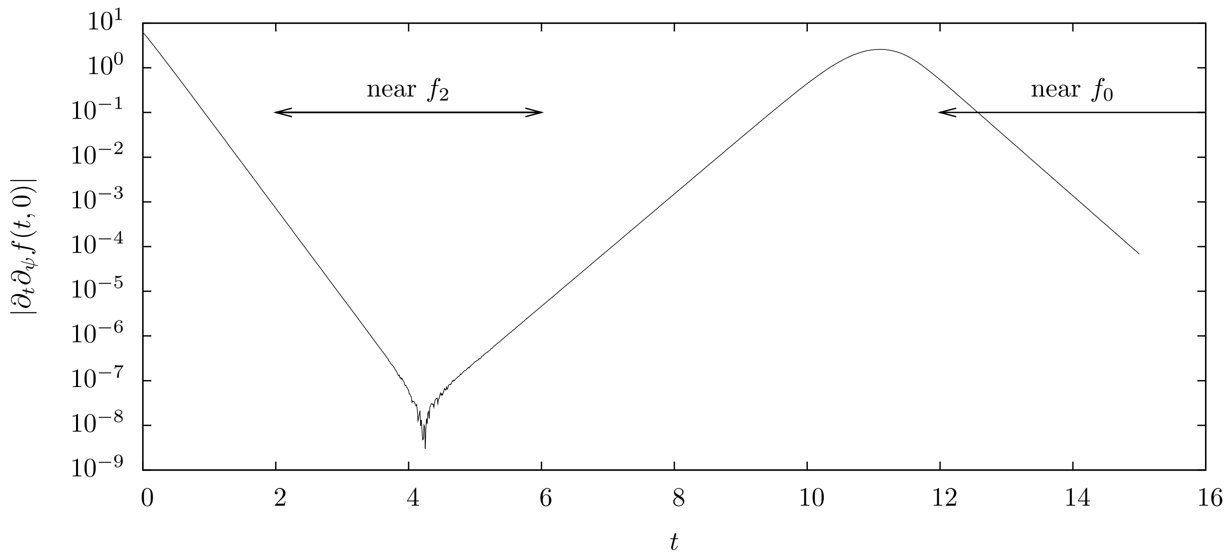


Figure 4.3: Stages of the heat flow evolution for symmetric initial data described in the caption of figure 4.1.

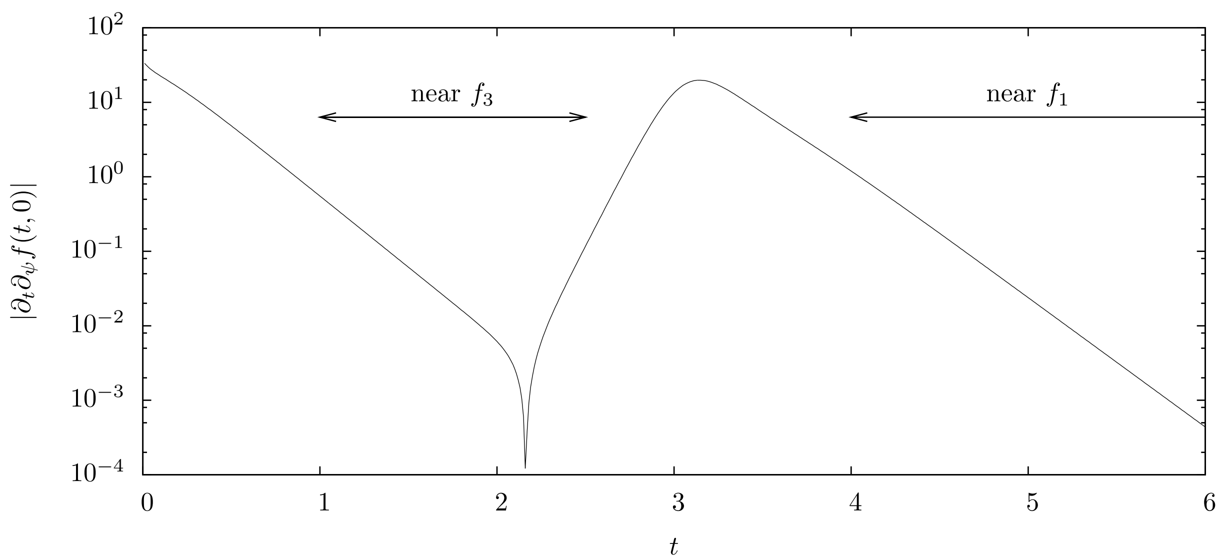


Figure 4.4: Stages of the heat flow evolution for antisymmetric initial data as described in the caption of figure 4.2.

# Appendix A

# Useful identity

Given the E-L equations

$$\frac{1}{w}\left(wf'\right)' + V(f,x) = 0 \tag{A.1}$$

the second variation in the direction $v = gf'$, for $g$ arbitrary, can be written as

$$\frac{1}{w}\left(wv'\right) + \frac{\partial V}{\partial f}v = \frac{1}{g}\left[\left(\left(\frac{g}{w}\right)' w\right)' v - \frac{\partial}{\partial x}\left(g^2 V(f,x)\right)\right] = A(x)v + B(f,x). \tag{A.2}$$

Where we have differentiated the E-L equation, multiplied it by $g$ and used the fact that

$$\frac{1}{w}\left(w(gf')'\right)' - g\left(\frac{1}{w}(gf')'\right)' = \left(\left(\frac{g}{w}\right)' w\right)' f' - 2g'V(f,x). \tag{A.3}$$

# Appendix B

# Numerical methods

## B.1 Method of lines

In order to solve the Cauchy problem

$$\partial_t f = \tau(f), \quad f(0,\psi) = g(\psi) \tag{B.1}$$

we discretize the spatial domain in a uniform way to create the grid of $N$ points

$$\psi_i = \frac{i-1}{N-1}\pi \in [0,\pi], \quad i \in 1,\dots,N. \tag{B.2}$$

To each point we assign a function of time $f_i(t)$, and we denote the set of $f_i$ as a vector $\vec{f} \in \mathbb{R}^N$. Then, the solution to (B.1) at points $\psi_i$ can be approximated by $f_i(t)$ if $\vec{f}$ is a solution to the following ordinary differential equation

$$\frac{d\vec{f}}{dt} = \hat{\tau}(\vec{f}), \quad f_i(0) = g(\psi_i). \tag{B.3}$$

The map $\vec{\tau} : \mathbb{R}^N \to \mathbb{R}^N$ is a discretized approximation of $\tau$. As $\tau = \tau(f, \partial_\psi f, \partial_{\psi\psi} f)$ it is sufficient to choose the differentiation schemes approximating the first and second derivatives. We choose the following discretizations of derivatives called the three point stencil

$$\partial_\psi f\big|_{\psi_i} \approx D_i \vec{f} = \frac{1}{2h}(f_{i+1} - f_{i-1}), \tag{B.4}$$

$$\partial_{\psi\psi} f\big|_{\psi_i} \approx D_i^2 \vec{f} = \frac{1}{h^2}(f_{i+1} - 2f_i + f_{i-1}), \tag{B.5}$$

where $1 \geq i \geq N-1$. We do not define the $D_0$, $D_N$ etc. because the boundary values imply $df_0/dt = 0$ and $df_N/dt = 0$ so we don't need the approximations of $\tau(f)$ at points $\psi_0$ and $\psi_N$. The above schemes are of order 2 and 1 respectively, which means that

$$\partial_\psi f\big|_{\psi_i} = D_i\vec{f} + \mathcal{O}(h^2), \tag{B.6}$$

$$\partial_{\psi\psi} f\big|_{\psi_i} = D_i^2\vec{f} + \mathcal{O}(h). \tag{B.7}$$

With such choice of differentiation schemes we end up with a following form of (B.3)

$$\frac{df_i}{dt} = \tau(f_i, D_i\vec{f}, D_i^2\vec{f}), \quad f_i(0) = g(\psi_i). \tag{B.8}$$

We solve the above equation using a Runge-Kutta method with adaptive step size described in the next section.

## B.2 Time marching method

To approximate the solution to the initial value problem for ordinary differential equation

$$y'(t) = f(t, y(t)), \quad y(0) = y_0 \tag{B.9}$$

where $y \in \mathbb{R}^N$ and $f : \mathbb{R} \times \mathbb{R}^N \to \mathbb{R}^N$ we use the explicit Runge-Kutta method with $s$ intermediate steps which approximates $y_{n+1} = y(t_{n+1})$ by

$$y_{n+1} = y_n + h\sum_{i=1}^{s} b_i k_i, \tag{B.10}$$

where $k_i$ are the values of the intermediate steps given by

$$\begin{aligned} k_1 &= f(t_n, y_n), \\ k_2 &= f(t_n + c_2 h, y_n + a_{21}k_1), \\ &\vdots \\ k_s &= f(t_n + c_s h, y_n + \sum_{j=1}^{s-1} a_{sj}k_j). \end{aligned} \tag{B.11}$$

The choice of the constants $c_i$, $a_{ij}$ and $b_i$ uniquely determines a specific Runge-Kutta (RK) method, there is also a systematical way of presenting those coefficient called the Butcher's tableau (table B.1).
To calculate the solution in an efficient way one can vary the time step size $\Delta t_n = t_{n+1} - t_n$ to decrease the number of calculations per a unit of time, keeping the relative error constant per unit of time. This is realized by combining two $s$-stage RK methods, one of order $p$ and the other of order $p+1$ which use the same intermediate values $k_i$, so having the same parameters $c_i$ and $a_{ij}$ but different $b_i$. The solutions are then approximated by

$$y_{n+1} = y_n + h\sum_{i=1}^{s} b_i k_i, \quad y^*_{n+1} = y_n + h\sum_{i=1}^{s} b^*_i k_i, \tag{B.12}$$

$$
\begin{array}{c|ccccc}
0 & & & & & \\
c_2 & a_{21} & & & & \\
c_3 & a_{31} & a_{32} & & & \\
\vdots & \vdots & \vdots & \ddots & & \\
c_s & a_{s1} & a_{s2} & \cdots & a_{s,s-1} & \\
\hline
 & b_1 & b_2 & \cdots & b_{s-1} & b_s
\end{array}
$$

Table B.1: The Butcher tableau for the explicit Runge–Kutta method.

where stars have been used to denote the coefficients of the method of order $p+1$. The difference between $y_{n+1}$ and $y_n$ gives the error estimate

$$\epsilon_i = |(y_{n+1})_i - (y^*_{n+1})_i| = h \left| \sum_{j=1}^{s} (b_j - b^*_j)(k_j)_i \right|, \quad i \in \{1, \ldots, N\}. \tag{B.13}$$

If the calculated error or too small compared with the desired error level the method changes step accordingly to the algorithm described in [5]. The method of our choice was embedded Runge–Kutta–Fehlberg (RKF45) of order 4/5 with the Butcher tableau presented in table B.2.

| | | | | | |
|---|---|---|---|---|---|
| 0 | | | | | |
| 1/4 | 1/4 | | | | |
| 3/8 | 3/32 | 9/32 | | | |
| 12/13 | 1932/2197 | -7200/2197 | 7296/2197 | | |
| 1 | 439/216 | -8 | 3680/513 | -845/4104 | |
| 1/2 | -8/27 | 2 | -3544/2565 | 1859/4104 | -11/40 |
| 25/216 | 0 | 1408/2565 | 2197/4104 | -1/5 | 0 |
| 16/135 | 0 | 6656/12825 | 28561/56430 | -9/50 | 2/55 |

Table B.2: Butcher tableau for embedded Runge-Kutta-Fahlberg method. The lowest row contains $b_i^*$.

# Bibliography


[1] P. Bizon and T. Chmaj. Harmonic maps between spheres. *Proceedings of the Royal Society A: Mathematical, Physical and Engineering Sciences*, 453(1957):403–415, February 1997.

[2] K. Corlette and R. M. Wald. Morse Theory and Infinite Families of Harmonic Maps Between Spheres. *Communications in Mathematical Physics*, 215(3):591–608, January 2001.

[3] J. Eells, Jr., and J. H. Sampson. Harmonic Mappings of Riemannian Manifolds. *American Journal of Mathematics*, 86(1):109 – 160, 1964.

[4] H. Fan. Existence of the self-similar solutions in the heat flow of harmonic maps. *Science in China Series A: Mathematics*, 42(2):113–132, February 1999.

[5] M. Galassi. *GNU Scientific Library Reference Manual (3rd Ed.)*. Network Theory Ltd.

[6] F. W. J. Olver, D. W. Lozier, R. F. Boisvert, and C. W. Clark, editors. *NIST Handbook of Mathematical Functions*. National Institute of Standards and Technology, Maryland.

[7] M. Reed and B. Simon. *Methods of modern mathematical physics, vol 4*. Academic Press, inc., London, 1972.

[8] M. Struwe. Geometric evolution problems. *Proceedings of 1992 graduate summer school*, pages 259—-339, 1996.